"Molded" Macroporous Poly(glycidyl methacrylate-*co*-trimethylolpropane trimethacrylate) Materials with Fine Controlled Porous Properties: Preparation of Monoliths Using Photoinitiated Polymerization

Camilla Viklund, Einar Pontén, Börje Glad,[†] and Knut Irgum*

Department of Analytical Chemistry, Umeå University, S-901 87 Umeå, Sweden

Per Hörstedt

Department of Pathology, Umeå University, S-901 87 Umeå, Sweden

Frantisek Svec[‡]

Cornell University, Department of Chemistry, Baker Laboratory, Ithaca, New York 14853-1301

Received May 29, 1996. Revised Manuscript Received September 25, 1996[⊗]

A model system has been developed for in situ photopolymerization of glycidyl methacrylate and trimethylolpropane trimethacrylate, leading to macroporous monolithic sorbents. This model system allows the preparation of continuous porous objects intended for applications such as detection, separation, and catalysis. The ease of the preparation, the short time needed for reaction, and the possibility of running the reaction at a low temperature are some of the main advantages of the photoinitiated in situ polymerization compared to a thermally initiated polymerization. Important system variables acting upon the porous properties and flow characteristics of the monoliths have been investigated in an experimental 2^3 full factorial design. The porous properties of the monoliths are a direct consequence of the quality of the porogenic solvent, as well as the percentage of cross-linking monomer and the ratio between the monomer and porogen phases. The presence of interactive effects between these reaction conditions were verified using multivariate analysis. It was concluded that the pore formation mechanism in an in situ photopolymerization follows rules similar to those found earlier for thermally initiated in situ polymerization of poly(glycidyl methacrylate-*co*-ethylenedimethacrylate) and poly(styrene-*co*-divinylbenzene).

Introduction

For decades, macroporous polymers have been used in a variety of analytical applications including chromatographic separation media, supports for catalysts, solid phase reagents, adsorbents, and in detection. These materials have primarily been produced as spherical beads by suspension polymerization, but other forms, such as macroporous membranes and disks, have also been reported.[1] A new type of macroporous sorbent, prepared by in situ bulk polymerization, has recently been introduced as an attractive alternative to traditionally packed beds for various separation processes.[2] These sorbents are formed from a homogeneous mixture of monomers, solvents, and an initiator in a closed mold. Following free radical initiation, the growing polymer chains precipitate to form nuclei which subsequently grow into a continuous array of connected spheroid particles or microglobules as the polymerization proceeds.

The monomer systems tested so far in this process include mixtures of styrene[3−5] and chloromethylstyrene[6] with divinylbenzene as well as glycidyl methacrylate[2,5,7−9] and acrylic acid[10] with ethylene dimethacrylate. The thermally induced homolytic decomposition of 2,2′-azobis(2-methylpropionitrile) has been used as radical source for the initiation of these polymerizations. Therefore, the reactions have to be carried out at elevated temperatures for 6−24 h.

The monoliths have been shown to offer an attractive alternative to packed beads for fast separation of proteins and peptides in the reversed-phase[3,4] or ion-exchange mode[2,7] and for the precipitation−redissolution chromatography of synthetic oligomers and polymers.[11] Some attempts have also been reported where thermal in situ polymerized sorbents have been used as substrates for molecular imprinting.[10]

[†] Present address: Astra Draco AB, Box 34, S-221 00 Lund, Sweden.

[‡] Present address: Department of Chemistry, University of California, Berkeley, CA 94720-1460.

[⊗] Abstract published in *Advance ACS Abstracts,* December 1, 1996.

(1) Svec, F.; Tennikova, T. B. *J. Chromatogr.* **1993**, *646*, 279.

(2) Svec, F.; Fréchet, J. M. J. *Anal. Chem.* **1992**, *64*, 820.

(3) Wang, Q. C.; Svec, F.; Fréchet, J. M. J. *Anal. Chem.* **1993**, *65*, 2243.

(4) Wang, Q. C.; Svec, F.; Fréchet, J. M. J. *J. Chromatogr.* **1994**, *669*, 230.

(5) Viklund, C.; Svec, F.; Fréchet, J. M. J.; Irgum, K. *Chem. Mater.* **1996**, *8*, 744.

(6) Wang, Q. C.; Svec, F.; Fréchet, J. M. J. *Anal. Chem.* **1995**, *67*, 670.

(7) Svec, F.; Fréchet, J. M. J. *J. Chromatogr. A* **1995**, *702*, 89.

(8) Svec, F.; Fréchet, J. M. J. *Chem. Mater.* **1995**, *7*, 707.

(9) Svec, F.; Fréchet, J. M. J. *Macromolecules* **1995**, *28*, 7580.

(10) Matsui, J.; Kato, T.; Takeuchi, T.; Suzuki, M.; Yokoyama, K.; Tamiya, E.; Karube, I. *Anal. Chem.* **1993**, *65*, 2223.

(11) Petro, M.; Svec. F.; Gitsov, I.; Fréchet, J. M. J. *Anal. Chem.* **1996**, *68*, 315.

S0897-4756(96)00301-8 CCC: $14.00 © 1997 American Chemical Society

Table 1. Physical Characteristics for ISPS Materials Prepared by Photoinitiated Polymerization According to the Factorial Design

	variables			responses				
exp	porogen/monomer[a]	TRIM/GMA[b]	isooctane/toluene[c]	D_p, mode[d] (nm)	D_p, mean[e] (nm)	V_p[f] (mL/g)	S[g] (m^2/g)	slope[h] (bar min/mL)
PGT1	70/30	70/30	70/30	4090	3600	2.5	18.6	2.6
PGT2	50/50	70/30	70/30	3430	3230	1.9	11.5	89.8
PGT3	70/30	30/70	70/30	4320	3280	2.3	16.1	2.5
PGT4	50/50	30/70	70/30	2760	2590	1.9	11.6	21.9
PGT5	70/30	70/30	30/70	454	225	3.0	87.2	1.4
PGT6	50/50	70/30	30/70	59	33	0.9	165	N/A
PGT7	70/30	30/70	30/70	6890	4900	3.0	8.3	2.3
PGT8	50/50	30/70	30/70	2050	1800	2.0	53.9	475
PGT9	60/40	50/50	50/50	5050	4530	2.1	10.3	10.1
PGT10	60/40	50/50	50/50	5080	4520	2.3	12.9	11.3
PGT11	60/40	50/50	50/50	4900	4540	2.0	18.1	13.1
PGT12	60/40	50/50	50/50	4990	4480	2.2	14.8	9.2

[a] Ratio between the porogens and the monomers in the polymerization mixture. [b] Ratio between the monomers (trimethylolpropane trimethacrylate and glycidyl methacrylate) in the monomeric mixture. [c] Ratio between the mixed porogens (isooctane and toluene) in the polymerization mixture. Initiation wavelength 365 nm; time for reaction 3600 s at ambient temperature. [d] Pore diameter at the highest peak in the pore size distribution curve. [e] Mean pore diameter. [f] Total pore volume. [g] Specific surface area. [h] Slope of the back-pressure vs flow rate curve.

A new application area for these sorbents stems from the fact that these monoliths, with their inherent potential of advantageous mass transfer to back-pressure ratio, constitute ideal carriers for heterogeneous reactions in chemical analysis. The reactivity of the accessible functional groups in these materials enables a broad range of chemical modifications of the sorbents. For example, in situ photopolymerized poly(glycidyl methacrylate-*co*-trimethylolpropane trimethacrylate) materials with immobilized luminophores have already been successfully used for detection of hydrogen peroxide at low concentrations in a peroxyoxalate chemiluminescence system.[12,13]

This report relates our systematic efforts to develop a photoinitiated in situ polymerized system for the preparation of monolithic sorbents based on glycidyl methacrylate and trimethylolpropane trimethacrylate. The principal aims of this study were to define the effects of the parameters that control the properties and to characterize these new materials, predominantly with respect to their porous structures and flow characteristics.

Experimental Section

Materials. The monomers trimethylolpropane trimethacrylate [TRIM] and 2,3-epoxypropyl methacrylate [glycidyl methacrylate, GMA] were of the highest purity available from Aldrich (Steinheim, Germany) and were freed from phenolic polymerization inhibitors by vigorous batch shaking overnight with the strong anion exchanger Amberlyst A-26 (≈0.1 g/mL monomer) in the chloride form.[14] The content of water in the monomers, verified by the Karl Fisher technique, were 0.3 and 0.02% (w/w), respectively. α-Methoxy-α-phenylacetophenone (benzoin methyl ether, 99%) and vinyltrichlorosilane (>97%) were purchased from Aldrich and Fluka (Buchs, Switzerland), respectively, and were used without further purification. Toluene (p.a., Merck, Darmstadt, Germany) and 2,2,4-trimethylpentane (isooctane, distilled, either from Burdick & Jackson or Fluka) were used as porogenic solvents. Pyridine was 99.5% pure from Riedel-de Haën (Seelze, Germany), tetrahydrofuran was of p.a. grade from Merck, and the absolute (99.5%) ethanol was from Kemetyl (Stockholm, Sweden).

Experimental Design and Data Analysis. Experiments were laid out in a 2^3 full factorial design with four center points. The variables included in the design were the porogen to monomer ratio, the cross-linker to functional monomer ratio, and the ratio between isooctane and toluene in the porogenic mixture (Table 1). The surface area, pore volume, most frequent pore size (mode), and the slope of the back pressure curve were chosen as responses. The experimental design was correlated with the results from the characterizations using the computer program MODDE 3.0 from Umetri AB, Umeå, Sweden. Partial least-squares (PLS) regression was used to evaluate both major effects and interaction terms. The quality of the model was ascertained by cross-validation. The predictive capacity Q_2 is a direct measure of the predictive power of the model with respect to the outcome of new experiments. In an attempt to improve the model, insignificant effects were removed stepwise until Q_2 was maximized. The visualized effects (Figure 2), however, correspond to the raw model with all variables included.

Choice and Pretreatment of Polymerization Tubes. Quartz glass tubes (38 mm long by 2.4 mm i.d., 4.1 mm o.d.) were etched by immersion in a saturated solution of ammonium hydrogen fluoride at room temperature for 15 min. After repeated washings with water, the tubes were dried in air at 80 °C for an hour, whereafter they were silanized by treatment with a solution containing dry pyridine, toluene, and vinyltrichlorosilane (molar ratio 9:5:1) at 50 °C for 6 h. The quartz tubes were washed consecutively with portions of acetone, water, and ethanol and allowed to dry at ambient conditions. Just prior to polymerization, the tubes were washed again with absolute ethanol and dried at 80 °C for 60 min.

Polymerization Procedure. The polymerization mixtures were prepared by weight by dissolving the initiator in the monomer mixture containing different amounts of GMA and TRIM. The porogen mixture, consisting of isooctane and toluene, was added to the monomers, and the solution sonicated in an ultrasonic bath (Bransonic 221) for 15 min. The sonicated polymerization mixture was purged with helium for 10 min, a process that resulted in <0.3% weight loss, regardless of the compositions. The mixture was then transferred to the quartz mold, which was sealed at the bottom by a PTFE plug protruding 5 mm into the tube. After filling, the upper end was sealed with a similar plug. In situ free radical polymerization was initiated by irradiating the upright standing filled quartz tubes for 60 min at room temperature in a Spectrolinker XL 1500 UV (Spectronics Corp., Westbury, NY) with eight 15 W fluorescent blacklight tubes (F15T8/BLB; GTE Sylvania), producing UV light of predominantly 365 nm wavelength. The built-in luminous power measurement facility of the XL-1500 indicated an intensity of 10 mW/cm^2 in the polymerization zone, but this was not an absolute value, since no attempts were made to calibrate this readout for the wavelength

---

[12] Pontén, E.; Viklund, C.; Irgum, K. *Anal. Chem.* **1996**, *68*, 4389.

[13] Stigbrandt, M.; Karlsson, A.; Irgum, K. *Anal. Chem.* **1996**, *68*, 3945.

[14] McGarvey, F. X.; Meunier, V. C.; Pollio, F. X. *Chem. Abstr.* **1963**, *48*, 13406c.

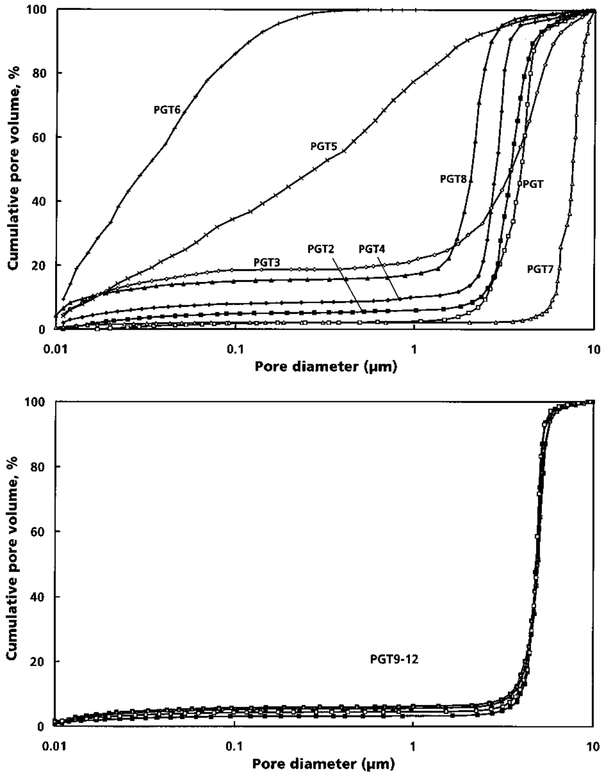

Figure 1. Cumulative pore size distribution curves for in situ polymerized poly(glycidyl methacrylate-*co*-trimethylolpropane trimethacrylate) monoliths. Conditions: λ = 360 nm; polymerization time 1 h at room temperature; polymerization mixtures according to the design PGT1−8 (upper), with center points PGT9−12 (lower) in Table 1.

employed. When the polymerization was complete, the plugs were carefully removed and replaced by similarly shaped end fittings that allowed the tubes with monoliths to be connected to test equipment. The porogen, unreacted monomers, and other soluble compounds were removed from the pores by washing with methanol (0.2 mL/min for 30 min) using an HPLC pump.

Pore Size and Surface Area Measurements. Prior to characterization of the porous properties, the in situ polymerized monoliths were removed from the tubes, cut into small pieces, Soxhlet extracted with methanol for 12 h, and dried in air at 80 °C for at least 3 days. The specific surface areas of the porous polymers were calculated from the adsorption/desorption isotherm of nitrogen using the BET equation, and the pore size distribution was determined by mercury intrusion porosimetry using an automated custom-made combined BET sorptometer−porosimeter (Porous Materials, Inc., Ithaca, NY).

Permeability of Porous Monoliths. The back-pressure was measured on a recorder which monitored the pressure output signal from a CMA 250 high-pressure pump (CMA/Microdialys, Solna, Sweden) while pumping absolute ethanol. The flow rate was varied from zero up to a maximum of 3 mL/min or a back-pressure of 10 MPa, whichever was limiting.

Electron Microscopy. All samples were placed on sticky carbon foils which were attached to standard aluminum specimen stubs. The carbon foils were used to increase conductivity. The samples were coated with approximately 20 nm of gold by using a combination of sputter coating (Edwards S150A sputter coating unit, Edwards High Vacuum, Crawley, UK) and evaporation (a modified Edwards E14 vacuum coating unit, Edwards High Vacuum, incorporating an automatic tilting and rotation device). Microscopic analysis of all samples was carried out in a S-360 iXP SEM (Leica Cambridge Ltd., Cambridge, UK) operated in LaB_6 mode, 5 kV, 100 pA probe current and 0° tilt angle. Final images were recorded from randomly chosen areas at 2000 and 4500 times magnification (only micrographs of the smaller magnification are shown in Figure 3).

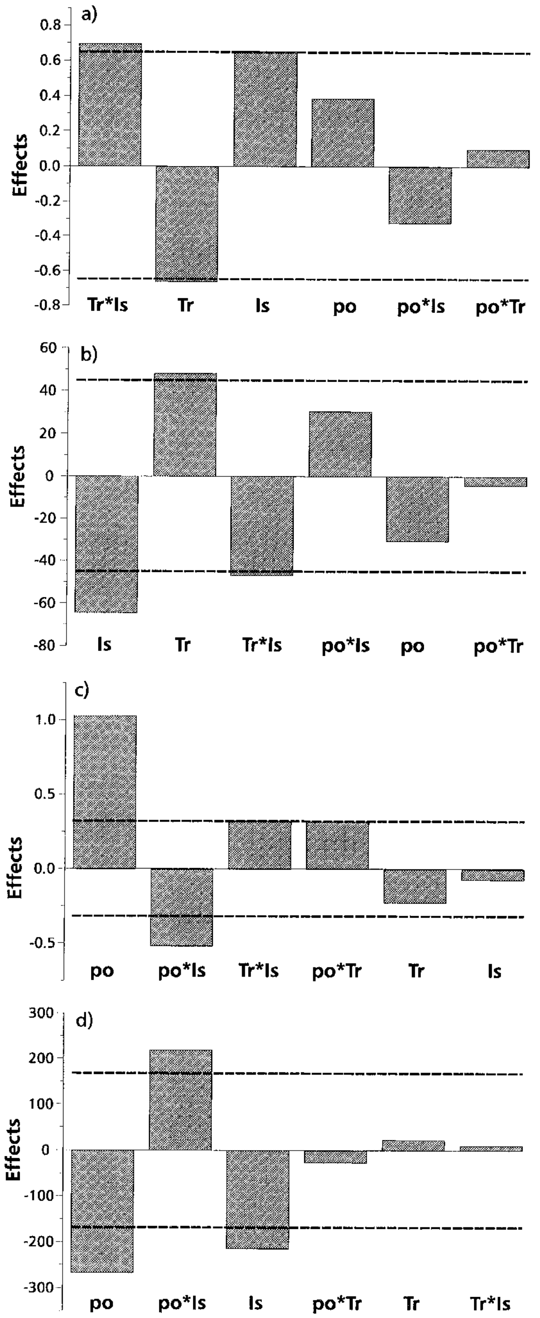

Figure 2. Effect plots for (a) log[pore $size_{mode}$], Q_2 = 0.12, R_2 = 0.84, N (number of experiments) = 12, DF (degrees of freedom) = 5; (b) surface area, Q_2 = 0.08, R_2 = 0.87, N = 12, DF = 5; (c) pore volume, Q_2 = 0.44, R_2 = 0.95, N = 12, DF = 5; (d) slope of the back pressure vs flow rate, Q_2 = 0.47, R_2 = 0.89, N = 12, DF = 5. po, porogen admixture; Is, isooctane to toluene ratio in the porogen mixture; Tr, TRIM/GMA ratio in the monomer mixture. The dashed horizontal lines describe the 95% confidence interval, and bars extending beyond these lines are significant at this level.

Results and Discussion

General Aspects upon the Choice of Polymerization Conditions. *Photoinitiation.* To our knowledge, photoinitiation has never been used for the preparation of continuous monolithic sorbents by polymerization in closed molds. In general, the polymerization is brought to completion more quickly compared with a thermally initiated system. Thermally initiated radical polymerizations are typically allowed to proceed for 6−24 h, whereas our photopolymerizations are

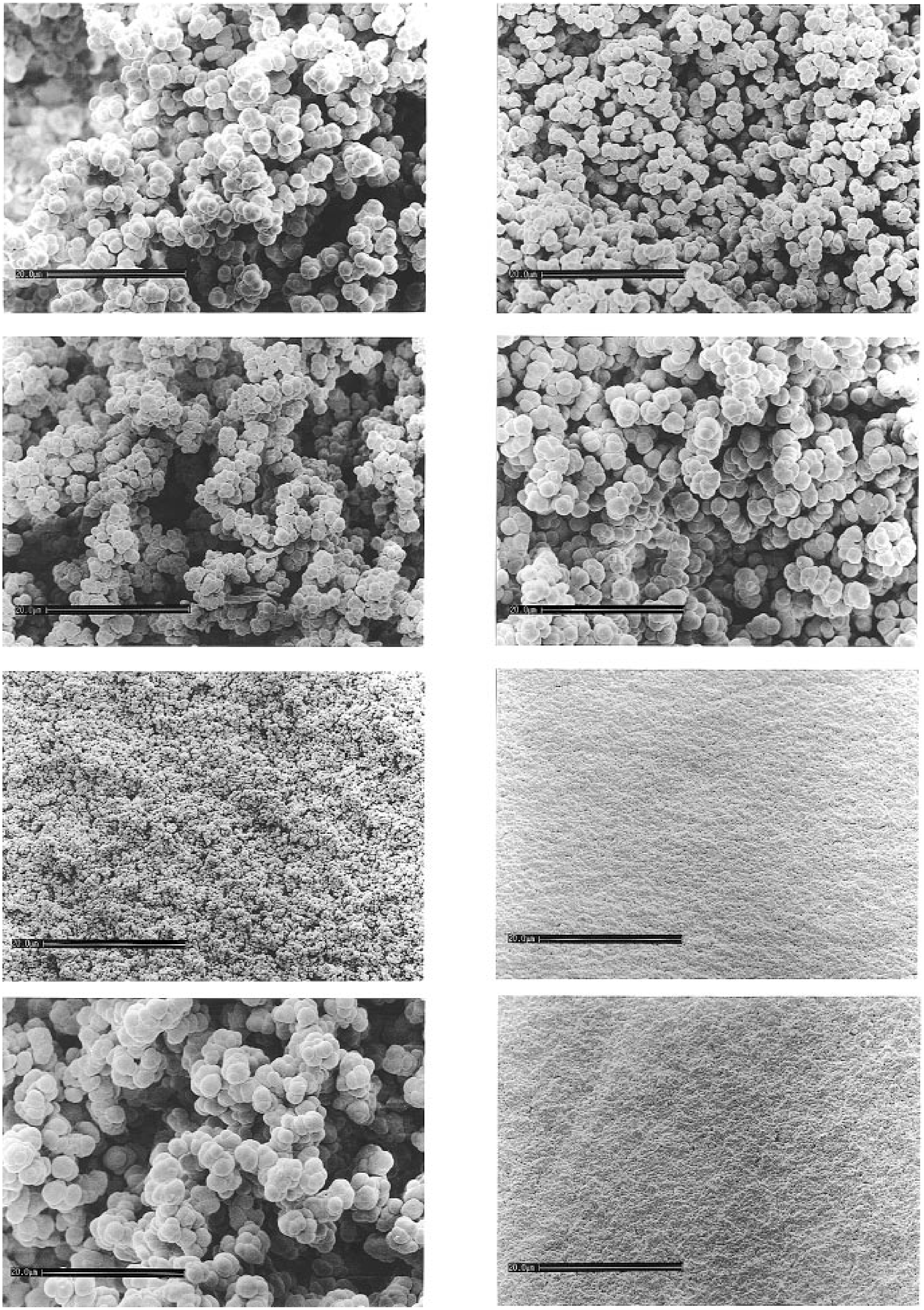

Figure 3. (a) Scanning electron micrographs of materials PGT1−8, arranged consecutively from PGT1 (left) and PGT2 (right) at the top to PGT7 and PGT8 (left and right, respectively) at the bottom. The scale bar in each micrograph represents 20 µm.

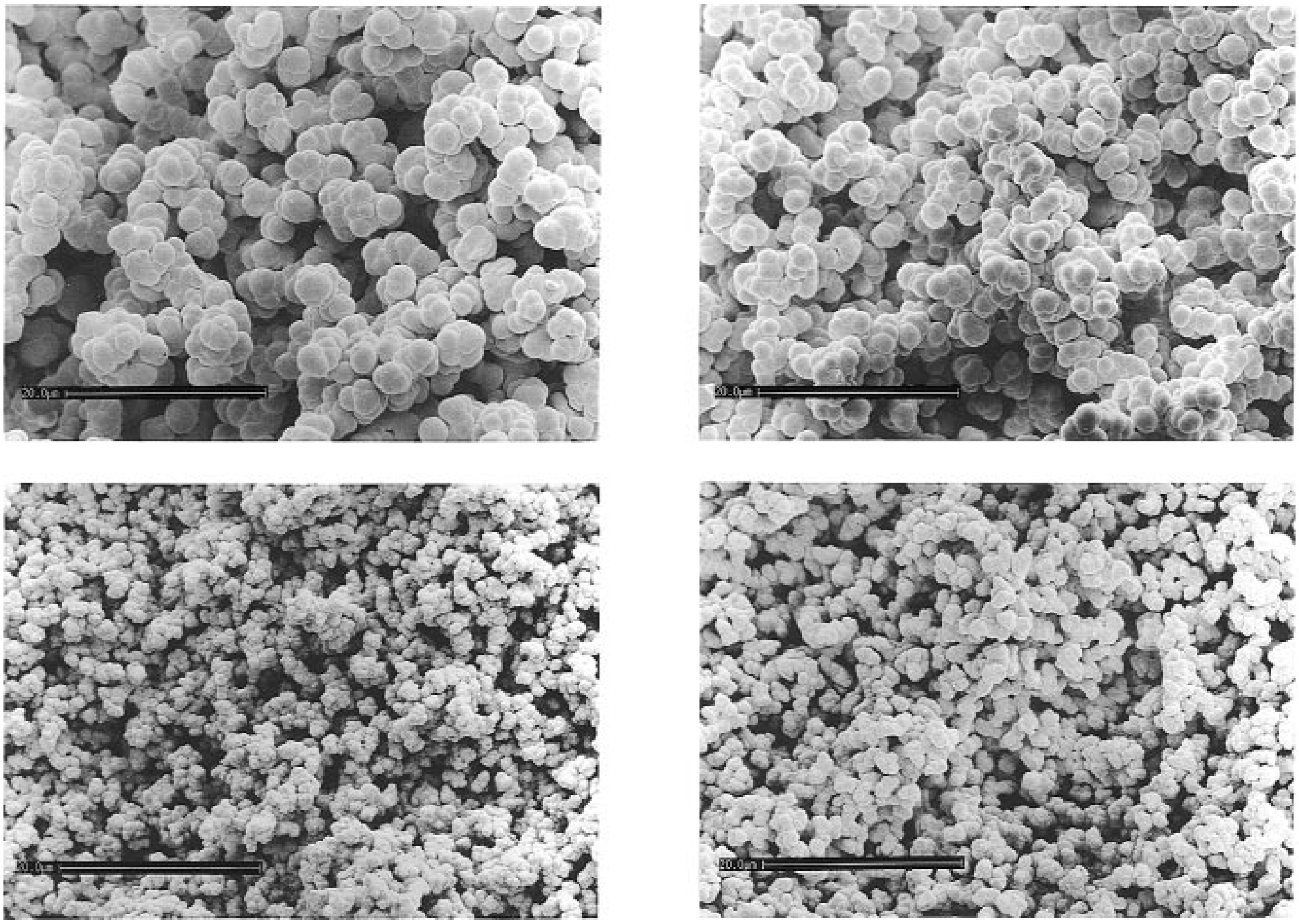

Figure 3b. Scanning electron micrographs of the center point experiments PGT9−12, scale and arrangement analogous to Figure 3a.

completed in less than 1 h. The fact that the polymerization runs at relatively low temperature is advantageous for the preparation of imprinted matrixes for molecular recognition.[10] It should however be noted that the temperature increases during the initial part of the polymerization process. It has been found earlier that the porous structure of thermally initiated polymerizations prepared in a vertically positioned cylindrical mold is partly influenced by gravity.[8] In the case of a fast photoinitiated polymerization, the gravity-related phenomena should be less apparent. Owing to the limited UV-light penetration depth, relatively thin polymerization reactors must be used to avoid radial gradients in the material. SEM studies carried out in the exploratory phase of this work verified that the morphology of a methacrylate-based monolith photopolymerized in situ within the confines of a closed PP tube with an internal diameter of 4 mm did not exhibit a visible radial gradient across the monolith surface.

Experimental Design. A screening study was first carried out to determine the most important parameters affecting the polymerization and pore formation process for the GMA/TRIM monomer system, to chart which parameters should be kept constant to obtain a reasonable number of experiments, and to establish the possible ranges of the selected variables for a full factorial design.

The free-radical photoinitiator benzoin methyl ether is commonly used in different photopolymerization systems.[15] As a result of our exploratory experiments, it was concluded that the benzoin methyl ether concentration should be about 1.5−2% (w/w) with respect to the monomers. An excessive coalescence of the microglobular structure, or even failure to polymerize, occurred at a concentration of less than 0.5%, while concentrations higher than about 3−4% led to cracks in the continuous polymer structure. The benzoin methyl ether concentration was therefore fixed at 1.5% in the experimental design.

Other important variables in photopolymerization are the intensity and wavelength of the light source. The intensity of the irradiation was kept constant at a level that yielded a fully developed monolith after 1 h of polymerization. The wavelength of the blacklight source is close to optimal for maximum photolytic cleavage of benzoin methyl ether.

The other variables included in this study include the percentage of porogen in the polymerization mixture, the composition of the porogenic solvent (toluene to isooctane ratio), and the cross-linker (TRIM) to reactive monomer (GMA) ratio. The latitudes of each of the variables, shown in Table 1, were confined to an experimentally suitable area, taking into account mechanical stability and flow permeability. The ranges were selected on the basis of experience gained in the preliminary experiments, so that a three-dimensional space could be spanned without practical problems and missing responses.

---

(15) Glad, B.; Irgum, K.; Hörstedt, P. *J. Membr. Sci.* **1995**, *101*, 53.

Polymerization Reactor. The surface modification procedure developed for the quartz tubes used as polymerization reactors involved bifluoride etching and attachment of a vinyl group to the surface by reaction with vinyltrichlorosilane. Although we have not been able to devise a technique that would objectively show the benefit of this treatment, our experience from a large number of polymerizations indicates that the wall adhesion increased markedly using this procedure.

Porous Properties of poly(GMA-*co*-TRIM) Monoliths. *Effect of Porogenic Solvent.* To obtain a rigid material that exhibits macroporosity, the polymerization mixture must contain large amounts of both cross-linking monomer and porogen. The porogen does not react during the polymerization process but remains within the pores, where it is surrounded by polymerized material, until finally removed during reaction workup. In most cases, the porogens are simple organic solvents or their mixtures. In this study we used mixtures of isooctane and toluene. Isooctane acts as a poor solvent for the growing polymer chains, while toluene is a good solvent with respect to the polymer.[16,17] Varying the ratio between these solvents thus alters the overall thermodynamic quality of the porogen. We noticed in our exploratory experiments that monoliths prepared with toluene only as porogen had extremely small pores, which made them almost useless in flow-through applications. Therefore, the experimental design (Table 1) was chosen to cover the range 30−70% of toluene, with isooctane balancing the porogenic mixture.

Table 1 indicates a close relationship between the thermodynamic quality of the porogenic solvent and the specific surface area. The higher the toluene/isooctane ratio, the higher the surface area. It should be noted that the specific surface area of a typical macroporous material is mainly due to the contribution from pores smaller than 50 nm (micropores and mesopores), while the contribution from larger pore families (macropores) is not substantial.[8] Focusing on larger pore sizes, it is seen in Table 1 that the most frequent pore size, representing the part of the distribution curve with the steepest slope as shown in Figure 1, was shifted toward smaller pores as the percentage of isooctane was decreased. In parallel, the increasing content of toluene resulted in an increase in the volume of the smaller pores (Table 1). The pore size distribution, which determines the specific surface area, can thus be controlled within a broad range by altering the thermodynamic quality of the porogen mixture.

It is apparent from Table 1 that the effect of isooctane/toluene ratio (with respect to surface area and/or mode of the pore size distribution curve) was observed for the total concentration of porogen at both the high and the low levels. The only exception to these observations was found for the experiment in which the percentage of porogen was at its highest level and the concentration of cross-linking monomer was at the low level (PGT7). However, these conditions are separately seen to decrease the specific surface area and/or increase the modal pore size (vide infra). It is important to recall that the mode (pore diameter at the highest peak in the pore size distribution profile for a monolith) and the specific surface area are measured by instrumental techniques which focus on different pore families, even if the data extracted by these two techniques are correlated. The presence of synergetic effects can further be suspected by noting the pore data for PGT6, for which the amount of porogen was at the low level while the level of cross-linker was high. These extreme conditions resulted in a monolith with a surface area far higher than all the other monoliths (165 m^2/g). Figure 1a and Table 1 reveal that this material was completely devoid of pores larger than 500 nm and that the majority of the pores turned out to be in the size range below 100 nm. This indicates that the percentage of both cross-linking monomer and porogenic solvent in the polymerization mixture affect the porosity in the same way as the thermodynamic quality of porogenic mixture. The effect of an increase in the percentage of toluene on the mode of the pore distribution curve was particularly striking at low porogen concentrations. The effect of the isooctane/toluene ratio upon the final flow characteristics of the monoliths is, furthermore, clearly consistent with the decrease in the slope (increased permeability) with increasing isooctane content discussed above.

A strong interrelation between the thermodynamic quality of the porogen and the pore formation process has already been established for both macroporous particles prepared by suspension polymerization[18−20] and thermally initiated monoliths.[5,8] Generally, the reaction medium consists of an initially homogeneous solution of monomer, porogen, and free radical initiator. Upon decomposition of the free-radical initiator, the growing polymers precipitate at some stage from the reaction mixture and form nuclei. The polymerization then continues both within the swollen nuclei and in the remaining solution to form microglobules. These grow further in size by coalescing with polymeric species from the reaction medium and by capture of newly precipitated nuclei. These growing units reach a stage when they are interconnected with each other by polymer chains threaded through neighboring microglobules, and larger agglomerates (clusters) of globules are formed. If the porogenic solvent is a good solvent for the polymer, phase separation will occur later and the solvent competes with the monomers in solvating the nuclei. Therefore, the concentration of monomer within the nuclei is relatively low, and the attraction between individual nuclei, resulting in coalescence, is limited. This leads to larger number of smaller microglobules, and the resulting pore size distribution is shifted toward smaller pores. Addition of the poor solvent (isooctane) to the polymerization mixture results in an earlier phase separation and swelling of the nuclei with the monomers remaining in the system is preferred. As a result, the formation of larger morphological units is promoted which translates into a formation of larger size of the voids.

Effect of Monomer to Porogen Ratio. The total amount of inert porogenic solvents in the polymerization mixture has to be controlled to ensure the formation of

---

[16] Reinholdsson, P.; Hargitai, T.; Isaksson, R.; Törnell, B. *Angew. Makromol. Chem.* **1991**, *192*, 113.

[17] Hargitai, T.; Reinholdsson, P.; Törnell, B. *J. Chromatogr.* **1993**, *630*, 79.

[18] Seidl, J.; Malinsky, J.; Dusek, K.; Heitz, W. *Adv. Polym. Sci.* **1967**, *5*, 113.

[19] Kun, K. A.; Kunin, R. *J. Polym. Sci.* **1968**, Pt. A-1, *6*, 2689.

[20] Guyot, A.; Bartholin, M. *Prog. Polym. Sci.* **1982**, *277*, 12.

porous structures with both pore size and pore volume which are sufficiently large to allow flow through operations at a reasonably low pressure. Table 1 shows that a decrease in porogen percentage in the system from 70 to 50% (PGT1 and 2) results in a decrease in the total pore volume from 2.5 to 1.9 mL/g. The peak corresponding to the mode of the pore size distribution profile is also shifted toward smaller pores (from 4.1 to 3.4 μm). As a direct consequence, the slope of the back pressure vs flow rate curve increases dramatically from 0.26 to 8.98 MPa min mL^{-1}. This result is supported by a similar univariate comparison that evaluates each pair of experiments $^3/_4$, $^5/_6$, and $^7/_8$ with respect to pore volume, permeability, and mode of the pore size distribution curve. For example, Table 1 documents that the mode of the distribution curve is shifted toward smaller pores as the porogen concentration decreases. The changes in these characteristics, which are obtained upon decreasing the percentage of porogen in the polymerization mixture, are mainly due to a decrease in the volume of large pores (>1 μm) and a parallel increase in volume of pores with sizes less than 50 nm (Table 1). However, if the level of isooctane is at the higher limit, the solvent quality effect is dominating and the amount of porogenic solvent is less critical.

An earlier study of thermally initiated “molded” polymerizations of styrenic and methacrylic systems[5] allowed us to establish a relationship between the pore size and the slope of the back-pressure vs flow rate dependency. A network of large channel-like pores in the range of 1 μm extending throughout the material is necessary to achieve high flow characteristics. Although not as consistent as with the thermally initiated monoliths, a similar correlation also applies for the photoinitiated poly(TRIM-*co*-GMA) monoliths (Table 1). It is evident that monoliths with the steepest increase in back pressure generally have low pore volumes. More notable, however, is the fact that monoliths prepared from two compositions (PGTs 2 and 5) deviate from this behavior in opposite directions. This seems to be due to synergy of different effects (vide infra).

When the concentration of TRIM is at its high level, the effect of a change in porogen percentage on the mode of the pore size distribution curve is relatively small. This is reasonable since, because of the high degree of cross-linking, it should be more difficult to create really large channels through a poly(TRIM-*co*-GMA) monolith.

Effect of Cross-Linking Monomer. The use of a trivinyl monomer for the preparation of a monolithic material should provide a higher degree of cross-linking in the final polymeric sorbent and ensure the high rigidity and mechanical stability necessary for application in a flow-through system. In exploratory experiments we concluded that TRIM concentrations above 75%, in combination with a high concentration of a good solvent such as toluene, yielded monoliths that were too brittle for our purposes. The lower limit chosen for the TRIM percentage in the polymerization mixture is limited by the mechanical stability of the polymer and the higher limit by the demand for reactive pendant epoxide groups in the sorbent. In the experimental design described in Table 1, the ratio between the cross-linking agent and the reactive monomer thus spans a TRIM content range from 30 to 70%.

Direct comparison of experiment pairs involving various amounts of cross-linker under otherwise identical conditions indicates that the effect of TRIM in the chosen interval was rather small for PGT1−4, which share a high content of isooctane in the porogenic solvent. It should also be noted, that PGT1 and -3 and PGT2 and -4 had pore volumes and surface areas that were very close to each other within each pair of experiments, while the modal pore size and the slopes of the back pressure vs flow rate lines were very close only for PGT1 and -3. For PGT2 and -4, the mode of pore size distribution curve decreases as the concentration of TRIM decreases.

However, the situation is completely different for PGT5−7. The mode for PGT5 and -7, prepared with 70 and 30% TRIM, respectively, and with a high level of porogen and a low level of isooctane, increases while the surface area decreases as the percentage of cross-linker decreases. The same results are found also for PGT6 and -8, where both the porogen concentration and the amount of isooctane in the polymerization mixture were at their low levels. Similar effects have earlier been observed in the thermally initiated preparation of poly (glycidyl methacrylate-*co*-ethylenedimethacrylate) and poly(styrene-*co*-divinylbenzene) monoliths.[5] This indicates that the pore formation mechanisms during photopolymerization used here follow the same rules as those which are typical for the thermally initiated polymerizations, despite the differences in temperature and polymerization kinetics.

Following the nuclei swelling argumentation above, an increased percentage of cross-linking monomer is likely to lead to an earlier phase separation of the formed polymer. A more highly cross-linked nucleus, however, will exhibit less tendency to swell with both solvent and monomer, and the sizes of the interconnected globules comprising the final porous structure should remain relatively small. The presence of more cross-linked nuclei will also decrease the tendency for the individual spheres to coalesce during polymerization and thereby prevent additional enlargement of microglobules.[5]

Multivariate Evaluation. Partial least-squares (PLS) analysis of multivariate data obtained from an experimental design yields information on the importance and effect of each variable included and is also superior regarding the determination of interactive effects between variables.[21] When several responses have been investigated in an experimental design, it is desirable to develop a model that describes the relationship of all the responses (Y matrix) to the included variables (X matrix). Using PLS analysis, it is possible to take all responses and their covariances into account in the model. The variables studied in the design are allowed to contain information that is partly overlaid. The fit of the model is determined by the R^2 value, which is the fraction of the response variation that is explained by the model. If the predictive capacity of the model (Q_2) is high, the model can be used for direct prediction of the outcome of new experiments. As a rule of thumb, the model contains such predictive information if the value of Q_2 is above 0.5.[21] By removing insignificant variables, the model can be improved and the predictive

---

(21) Lindgren, Å. Multivariate Structure−Property-Relationships of Non-Ionic Surfactants. Ph.D. Thesis, Umeå University, 1995.

capacity increased. Even with low values of Q_2, the model can be useful when unraveling convoluted effects, such as in the search for optimum conditions in the synthesis.

PLS analysis of the multivariate data has been carried out for each of the responses chosen. The effects of each variable and the two-way interactions between variables on each response are visualized in Figure 2. A logarithmic transformation was also used on the most frequent pore size (mode) due to the broad range of sizes spanned by the experiments. Values of predictive capacity (Q_2) and R_2 correspond with the nonoptimized model, where all variables are included regardless of their significance. This was done in order to visualize all effects simultaneously and decrease the risk of overestimating the model. By removing the insignificant factors, an optimized model can be obtained with predictive capacities of 0.24 (most frequent pore size$_{\mathrm{mode}}$, DF = 7), 0.29 (surface area, DF = 7), 0.63 (pore volume, DF = 6), and 0.65 (slope of the back-pressure curve, DF = 8). It should be noted that 50 MPa min mL^{-1} was used as back pressure slope value for PGT6, as it was impossible to measure the value accurately with the technique used.

When the mode of the pore size distribution curve was chosen as response (Figure 2a), the PLS analysis gave a result consistent with the univariate analysis, with pore sizes increasing with an increasing amount of isooctane in the porogenic mixture. The effect of TRIM is seen to have a large negative (decreasing) effect on the mode. This was, however, expected from the univariate evaluation. More interesting is the interaction between solvent quality and amount of TRIM. According to the model, the mode pore size increases as the percentage of isooctane at high levels of TRIM increases but slightly decreases with increasing isooctane content at low levels of TRIM. This visualizes the need for having a rigid, extensively cross-linked monolith to prevent collapse of very large pores in the dry state.

The main effect of TRIM on the specific surface area is shown in Figure 2b. As expected, the surface area increased as the percentage of cross-linking agent in the mixture increased. This leads to the conclusion that the same variables are of significant importance for the response in both surface area and mode of pore size distribution, although these properties vary inversely with each other. We have seen earlier the *main effect* of percentage of cross-linking agent in the polymerization mixture in the preparation of poly(glycidyl methacrylate-*co*-ethylenedimethacrylate) and poly(styrene-*co*-divinylbenzene) monoliths by thermally initiated polymerization.[5] The interaction between solvent quality and percentage of cross-linking monomer conceals the effect of the amount of isooctane at low concentrations of TRIM shown in Figure 2b.

The most interesting finding in the multivariate study is that the total pore volume of the dried polymers was not significantly increased when higher concentrations of isooctane were used. As can be seen in Figure 2c, the isooctane/toluene ratio was, in fact, the least important variable (with respect to the pore volume) included in this experimental design. The interaction study also showed the combined effect of the amount and quality of the porogen. Clearly, the effect of a decrease in the amount of porogen on the pore volume was more serious at higher levels of toluene. Figure 2c also shows that the variation in the content of isooctane on the total pore volume was influenced by the level chosen for TRIM.

From Figure 2d, it is evident that an increase in the percentage of porogen and a decrease in its thermodynamic quality had similar effects on the permeability of the monoliths to liquids. This is a reasonable result consistent with the univariate analysis. If the interaction between the quality and percentage of porogen is plotted, it can be seen that an increase in percentage of porogen in the polymerization mixture was less important when the amount of isooctane was at the high level.

Scanning Electron Microscopy. The effect of the polymerization variables on the textures of the dry poly(GMA-*co*-TRIM) monoliths is illustrated by the electron micrographs shown Figure 3a. In the typical network, microglobules of relatively uniform size were agglomerated to larger clusters. They do, however, largely retain their individuality.

Evaluation of SEM visible effects of the various design parameters on the particle texture indicates that solvent quality had the most prominent impact on the morphology. A comparison of the experiment pairs PGT1 and -5 and -4−8 substantiates the dominant effect of the solvent quality, with large macropores at low toluene content, in contrast to materials involving only mesopores and micropores at the high toluene level. Notable is PGT7, which markedly deviates from this pattern. This experiment reveals the two most important interaction effects, i.e., those of percentage of porogen and solvent quality and of solvent quality and percentage of TRIM in the system, which lead to prediction of larger pores in the PLS evaluation. The micrograph shows extremely large pores located between the agglomerates. This confirms the high permeability for liquid observed for this monolith. The size of the microglobules is in the range 1−2 mm. The SEM study also verifies that the porous structure of polymers characterized with surface areas above 54 m^2/g (PGT5, -6, and -8) consists of microglobules at least 1 order of magnitude smaller than those typical of monoliths having lower surface areas.

In general, there is a reasonable correlation between morphology and porous properties with the exception of PGT8, for which the pore size distribution curve shows mode at 2 μm. Quite surprisingly, the SEM micrograph does not show signs of pores in that size range, and the synthesis was therefore repeated and the pore distribution characterized, with identical result. The BET and back-pressure measurements verify the dense structure seen in the SEM picture for PGT8.

The most spectacular sorbent in this series was PGT5, with a modal pore size of 0.45 μm and a surface area of 87 m^2/g. This monolith exhibits the lowest back-pressure of the entire design. The cumulative pore size distribution for this monolith (Figure 1a) exhibited pores that span a very broad range, so that the material contains both very large and smaller pores to a much larger extent than the other materials. The SEM study also verifies the special nature of PGT5, a highly porous structure consisting of medium size microglobules, not involving pores larger than 1 μm. Evidently, by using the approach of experimental design and multivariate analysis, we have been able to find several unique monolith compositions within an experimental domain that may seem relatively narrow. Chemometrics have thus proved to be an excellent tool when designing new polymeric materials.

Conclusion

Photopolymerization offers a viable alternative route for the rapid in situ preparation of macroporous polymeric monoliths suitable as sorbents in analytical chemistry. The physical characteristics of photopolymerized poly(glycidyl methacrylate-*co*-trimethylolpropane trimethacrylate) can be controlled by changing the composition of the polymerization mixture. Interactive effects between polymerization variables could be identified and explored using multivariate analysis of the physical properties. The secondary interaction between the amount and quality of the porogen, as well as between the porogen quality and the TRIM/GMA ratio, was of a surprising importance for the porous properties of poly(GMA-*co*-TRIM). Using optimized conditions, materials having high surface area, low flow resistance and good mechanical stability can be prepared, thus yielding sorbents which are suitable for a broad variety of analytical applications.

Acknowledgment. This work was supported by The Swedish Natural Science Research Council through Grant K-KU 8724-309 et seq., by Grant GM 48364-04 from the National Institute of Health, and by scholarships from The Bengt Lundqvist Memorial Foundation (C.V. and E.P.). Its legibility has benefitted from the linguistic scrutiny of Michael Sharp.

CM9603011